Document downloaded from:

http://hdl.handle.net/10251/183529

This paper must be cited as:

Molina-Gomez, NI.; Varon-Bravo, LM.; Sierra-Parada, R.; López Jiménez, PA. (2022). Urban growth and heat islands: A case study in micro-territories for urban sustainability. Urban Ecosystems. 1-19. https://doi.org/10.1007/s11252-022-01232-9

The final publication is available at

https://doi.org/10.1007/s11252-022-01232-9

Copyright Springer-Verlag

Additional Information

Urban growth and heat islands: A case study in micro-territories for urban sustainability

Nidia Isabel MOLINA-GÓMEZ,[a* 1], Laura Marcela VARON-BRAVO[a 2], Ronal SIERRA-PARADA [a 3], P. Amparo LÓPEZ-JIMÉNEZ[b 4]

[a] Department of Environmental Engineering, Universidad Santo Tomás, INAM-USTA, Carrera 9 51-11, 110231 Bogotá, Colombia

[b] Hydraulic and Environmental Engineering Department, Universitat Politècnica de València, Camino de Vera, 46022 Valencia, Spain

*Corresponding author

1. *e-mail*: frauisabel@gmail.com; nidiamolina@usantotomas.edu.co; ORCID: 0000-0003-4485-262X
2. *e-mail:* lauravaron@usantotomas.edu.co; ORCID: 0000-0002-4091-3424
3. *e-mail:* ronalsierra@usantotomas.edu.co; ORCID: 0000-0002-9206-5682
4. *e-mail:* palopez@upv.es; ORCID: 0000-0002-7043-3683

Abstract

Rapid urbanization contributes to the development of phenomena such as climate variability, especially in tropical countries, which negatively impact ecosystems and humans, factors that influence urban sustainability. Additionally, the increase of building construction prevents the flow of wind streams contributing to the retention of pollutants and hot air masses, causing events such as urban heat islands (UHI). This study aimed to analyze from the micro-territorial level, the influence of urban growth on the UHI phenomenon over the last two decades (2000-2020) in the locality of Kennedy, in Bogotá, Colombia. For this purpose, environmental and socio-economic

factors were evaluated. For the former, Landsat satellite images and spectral indices were used to evaluate the spatial-temporal variation in the quantity and quality of vegetation, bodies of water, urbanized areas, impervious surfaces, as well as to calculate the land surface temperature and its distribution in the study area. With regard to the socio-economic factors, the variables considered for analysis were population density and energy consumption. Lastly, a principal component analysis was carried out to identify possible associations between the variables and to identify the contribution of each micro-territory to the UHI phenomenon in the study area. The spatio-temporal variations reveal a growing trend over time, especially in impermeable areas where several economic activities, vehicular traffic, and population density converge, which require certain actions to be prioritized in territorial planning and the addition of public green spaces in urban zones.

Keywords: Urban heat island; land surface temperature; spectral indices; remote sensors; principal component analysis; micro-territories.

1 Introduction

The world's population has increased exponentially, and this trend will continue, especially in areas such as Asia, Africa, and Latin America. It was estimated that in 2018, 55% of people lived in cities and this figure is projected to increase by 13% by 2050 (United Nations, 2019). Therefore, there will be increased population density, the expansion of settlements, land cover changes, increased energy consumption, pollution, and the modifications of cities' microclimates, which include the urban heat island phenomenon (UHI) (Singh, Kikon, & Verma, 2017).

A UHI is an effect that hinders urban sustainability. The latter can be evaluated from factors that describe the environmental, social, and economic behavior of territories (Shen, Kyllo, & Guo, 2013). The environmental dimension includes factors related to air quality, biodiversity, water, and soil resources. The social dimension encompasses population growth, health-related effects on the

inhabitants, in addition to social conditions regarding access to services related to urban expansion and densification. Lastly, the economic dimension entails infrastructure as support for territorial development and consumption patterns (United Nations, 2007), including energy consumption. In the context of this study, these are major interrelated components and are part of the Sustainable Development Goal (SDG) known as sustainable cities and communities (UNDP, 2020).

UHI refer to the temperature difference between urban and rural areas (Amanollahi, Tzanis, Ramli, & Abdullah, 2016; Estoque & Murayama, 2017; Oke, 1982), which is inevitable in cities due to urbanization processes that include surfaces originally covered by vegetation being replaced by infrastructures such as roads, houses, and buildings, where the thermal mass built causes an increase of land surface temperature (LST) and the resulting UHI phenomenon (Carpio, González, González, & Verichev, 2020; Estoque & Murayama, 2017; Papparelli, Kurbán, & Cúnsulo, 2011; Singh et al., 2017). Moreover, UHI intensity rises with increasing urban occupancy (Papparelli et al., 2011).

As stated by Papparelli et al., (2011) and Rizwan, Dennis, & Liu, (2008), the increase in surface temperature is associated with anthropogenic activities which are the result of heat generated by vehicles, power plants, air conditioning, among other causes (Rizwan et al., 2008). Urban infrastructure absorbs this heat, as do atmospheric pollutants such as aerosols found in urban areas with high pollution levels (Rizwan et al., 2008). The increase in LST entails greater energy demand, which exacerbates air pollution, cardiovascular and respiratory diseases, and impacts humans' quality of life (Bokaie, Zarkesh, Arasteh, & Hosseini, 2016; Liu et al., 2020; Senanayake, Welivitiya, & Nadeeka, 2013; Zhou et al., 2019).

This phenomenon has been studied primarily in countries such as the United States, Germany, Greece, France, as well as in Asian countries such as China, India, and Japan, which have provided significant research on heat factors (Ulpiani, 2021; Zhou et al., 2019). Nevertheless, there is a lack of research on UHI in Latin America (Dobbs, Hernández-Moreno, Reyes-Paecke, & Miranda, 2018; Litardo et al., 2020; Peres, Lucena, Rotunno Filho, & França, 2018; Portela, Massi,

Rodrigues, & Alcântara, 2020; Wu et al., 2019), which is necessary due to continuous urbanization processes and increasingly intensifying climate sensitivity. Although urbanization processes generate effects in all territories, it is important to note that the urban growth rate in developing countries such as those in Latin America is 2.29% per year, compared to 0.47% in developed countries (United Nations, 2019).

Studies on UHI have been carried out primarily for areas larger than 100 km^2. However, it is noteworthy that in smaller areas, there may be alterations in the factors that influence UHI related to environmental, social, and economic dimensions, similar to those in capital cities such as in the city of Baguio, Philippines, which covers an area of 57.5 km^2 (Estoque & Murayama, 2017). Therefore, there is a need to promote studies on UHI in smaller areas, as they are more likely to experience drastic changes from the effect of urban warming (Zhou et al., 2019), and thus in their sustainability dimensions. A local resolution analysis could facilitate the precise identification of areas affected by this phenomenon, to establish a scheme to prioritize actions for its mitigation and contribute to the planning of sustainable cities from the micro-territory level.

In this research study, zonal planning units (ZPU) function as a spatial unit category (micro-territories) to understand both environmental and socio-economic factors, which may influence the formation of UHIs within the study area. The ZPUs were created through a decree in 2000 with the adoption of the Bogota Land Use Plan. In this manner, the micro-territories were conceived as an urban planning instrument that would enable development at the neighborhood level (Yunda & Sletto, 2020). ZPUs also facilitate the regulation of urban land in sectors with common elements in terms of land use and productive activities, building height, public space, and road conditions (Guzman, Gomez, & Rivera, 2017).

According to (Molina Jaramillo, 2018), the micro-territory category entails more than a spatial delimitation through administrative and/or socio-cultural boundaries. It also refers to the space where daily life takes place, which facilitates an analysis of the population's health and well-being

conditions at the neighborhood and community levels.

This study examines micro-territories as units of analysis within large cities, given that they facilitate the evaluation of different phenomena's behavior on a smaller scale, as well as the selection of measures with a synergic effect that can be applied in larger areas.

Therefore, this research study seeks to answer the following question: How does urban growth influence the manifestation of the urban heat island phenomenon at the micro-territorial level?

Studying UHI requires a technical analysis from the perspective of temporal and spatial changes, in addition to knowledge of LST distribution in areas that have gone through urbanization processes. Moreover, areas with unusual temperatures must be identified. Given its capacity to map thermal distribution, satellite image processing was used, as it enables the analysis of distributed LST at the spatio-temporal level (Senanayake et al., 2013).

The main objective of this work was to analyze from the micro-territorial level, the influence of urban growth on the UHI phenomenon over the last two decades (2000-2020). This study includes an association analysis of land use and land cover changes, mainly due to anthropogenic variables. To this end, this study developed a temporal analysis of the behavior of environmental and socio-economic factors, based on digital processing of satellite images and information provided principally by government entities.

Examining environmental factors includes analyzing spatio-temporal changes in vegetation along with the addition of build-up and impervious surfaces, by using spectral indexes to extract and calculate the built areas in terms of their shape, size and spatial context, namely: normalized difference vegetation index (NDVI), normalized difference built-up index (NDBI), and normalized difference impervious surface index (NDISI). It also includes the identification of water bodies and wetlands as represented in the normalized difference water index (MNDWI) and lastly, the calculation of the spatial distribution of land surface temperature (LST). Meanwhile, socio-

127 economic factors include population density and energy consumption in the analysis period as
128 factors that could influence the UHI phenomenon.
129 This study is innovative in that it recognizes the importance of a bottom-up approach,
130 developing a multiscale analysis in a territory with little vegetation, located near the equatorial zone
131 at an altitude of 2625 meters. The combination of the analysis of satellite images and census
132 information with statistical procedures performed, in order to identify the relationships of urban
133 growth, UHI, and sustainability in the micro-territory further highlights the contributions and
134 innovation of this research.
135 The procedure and results from this work will serve as an input for the analysis of the
136 influence of urban growth and meteorological variables on urban sustainability. Additionally, it will
137 make it possible to identify the specific contribution of micro-territories on the main components of
138 UHI using PCA. Lastly, it will serve as technical support for decision-makers in the field of
139 territorial planning. In the design and development of urban spaces, territorial planners should
140 recognize areas where environmental deterioration factors converge (changes in vegetation cover,
141 reduction of water bodies, increased LST) and their causes, which are the variables analyzed in this
142 study. In this manner, guidance can be provided regarding the best options to mitigate
143 environmental problems, in this case, the UHI phenomenon.
144

145 **2 Methods**

146 *2.1 Study area*

147 The locality of Kennedy was the territory selected for the case study; it is located in the
148 southwest of Bogotá, the capital of Colombia (see Fig.1) at an altitude of 2625 meters on a high
149 plateau on the eastern slopes of the Colombian Andes. According to the work done by Wu et al.
150 (2019), in which the authors made use of a medium resolution image radiometer spectrum, Bogotá
151 is one of the cities in Latin America with the highest daytime and nighttime UHI. Furthermore,

according to Ramírez-Aguilar and Lucas (2019), Kennedy has the most intense UHI in the city. The study area is characterized as a space lacking in vegetation tied to an urban transformation process accentuated in the west of the locality.

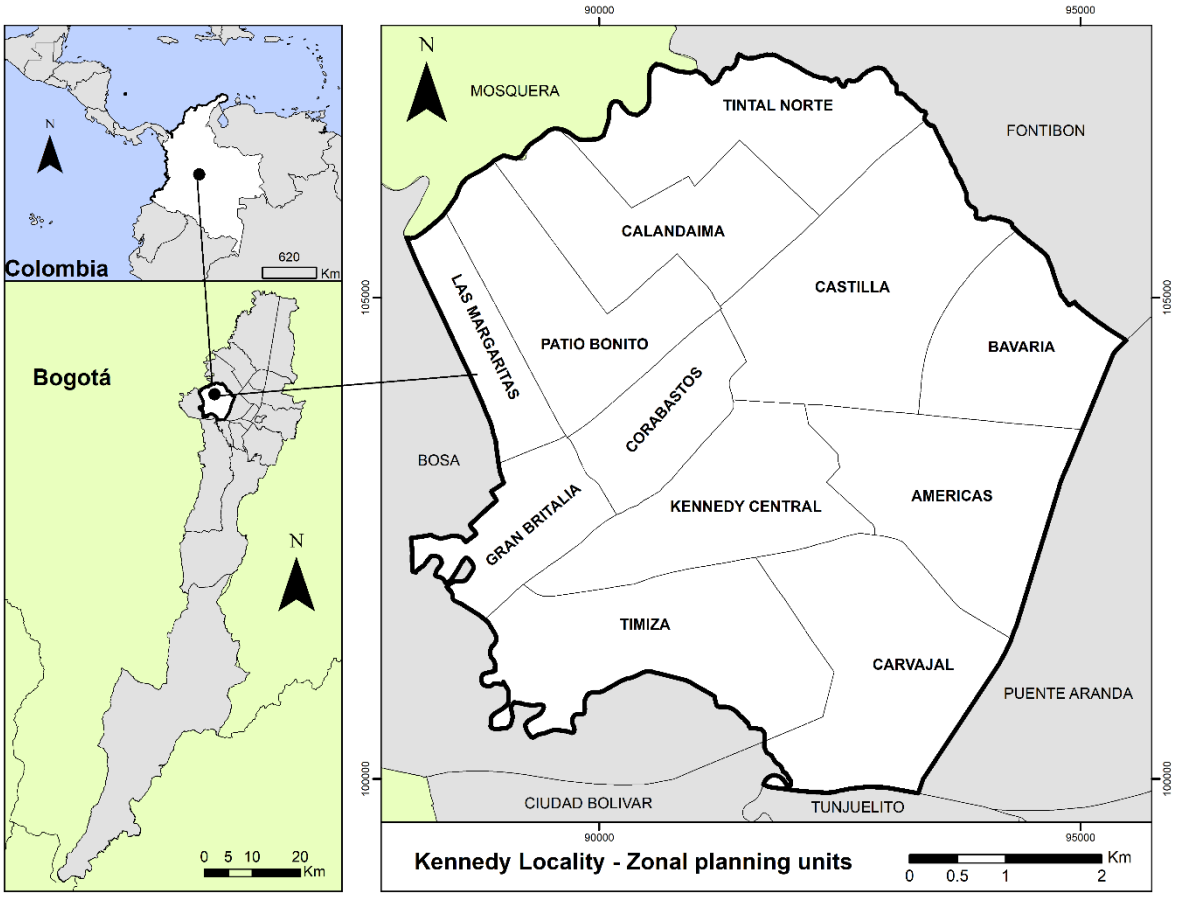

Fig. 1. Location of the study area

Kennedy is one of twenty localities in the capital city and is situated on a flat area where important water sources are found, such as the Bogota, Fucha, and Tunjuelo Rivers, along with the La Vaca, El Burro, and El Techo Wetlands.

In 2018, Kennedy had 1,230,539 inhabitants, approximately 15% of the city's total population, with an average population growth rate of 2.5% per year. The locality has a total area of 38.58 km^2, of which, 93.4% is urban, with 6.5% corresponding to urban expansion (Veeduría Distrital, 2018).

The locality is distributed into twelve zonal planning units (ZPU) (see Fig.1), which were implemented to better manage urban development planning. There are several economic activities in the locality including the city's main supply center. Kennedy has a system of public transportation portals and road infrastructure for access and transit in the city.

In 2012, according to government entities, most of the locality had an average buildability of 2 – 4 floors per block, and by 2020, the height increased to 4 – 5 floors in the ZPUs of Corabastos, Castilla, and Calandaima. The ZPUs of Bavaria and Castilla have specific points with buildings higher than 15 floors.

Meteorological data for the study area is monitored by the Carvajal Sevillana station located to the south of the locality (in the Carvajal ZPU) and the Kennedy station in the Kennedy Central ZPU. During the period from 2008–2019, annual average surface temperatures of 15.4°C and 14.9°C were recorded by the Carvajal Sevillana and Kennedy stations, respectively (SDA, 2020).

Concerning the average accumulated precipitation, during 2008–2019, the Carvajal station recorded 725.7 mm with the Kennedy station logging 828 mm. On average, the months with the most rainfall in 2019 were May, October, and November. The first and third quarters of the year registered the lowest rainfall (SDA, 2020).

Kennedy is a city sector with environmental and socio-economic characteristics that make it relevant for an analysis of urban sustainability. It is the second most populated locality in the city and has the most significant problems in terms of air quality (Ramírez-Aguilar and Souza, 2019). During 2016–2019, the WHO recommendation (2006) for PM_{10} ($50\mu g/m^3$) was exceeded by an annual average of 220 days at the Carvajal-Sevillana station, and 165 days at Kennedy station. The largest exceedances are historically during the first quarter of the year (SDA, 2020).

2.2 Research design

To achieve the research objective, a methodology consisting of the following five sequentially developed stages was used (see Fig.2): 1) information gathering and image processing; 2) calculation of spectral indices; 3) calculation of LST; 4) analysis of the UHI phenomenon; and 5) analysis of the relationship between the variables and UHI. The development of these stages sought to determine the degree of association between the selected environmental and socio-economic variables and in turn, explain the correlation between urban growth and the UHI phenomenon. The stages are described below.

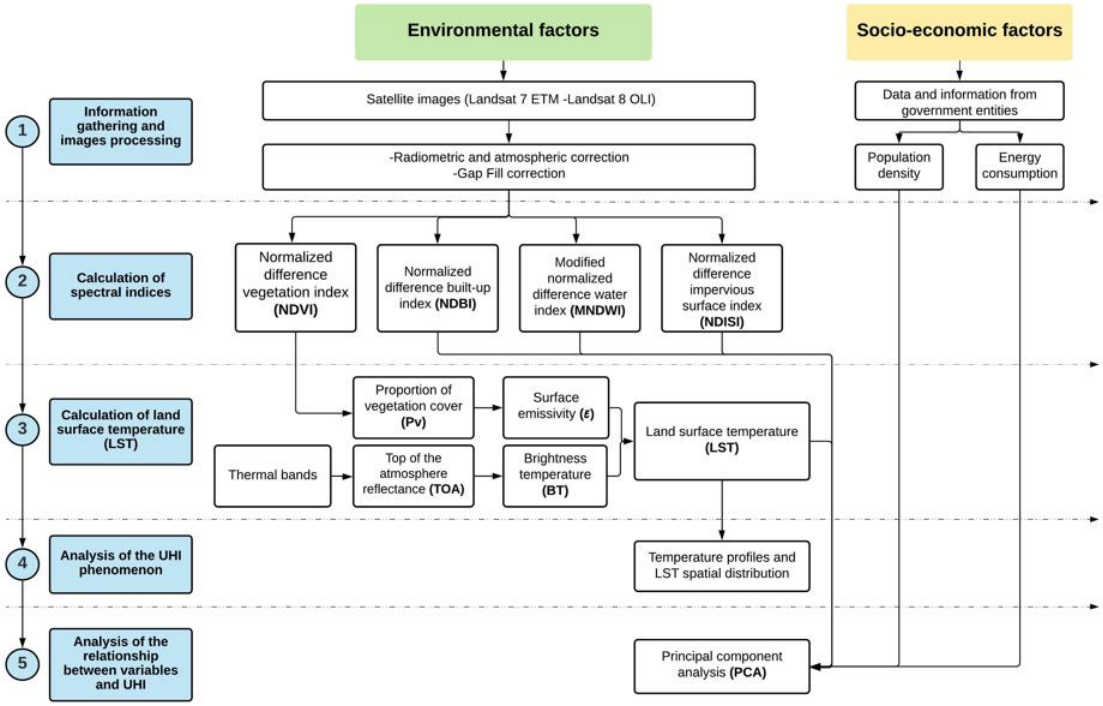

Fig. 2. Procedure to analyze the influence of urban growth on the UHI phenomenon.

2.2.1 Information gathering and image processing.

This stage entails gathering information on environmental and socio-economic factors. Regarding environmental factors, information was gathered from satellite images; meanwhile, for

socio-economic factors, information was compiled from data recorded by governmental entities, including census information.

Environmental factors

Several available satellite missions currently have accessible information to develop multi-temporal studies of urban phenomena, with the US Geological Survey (USGS) Landsat Mission being one of the few which provide its services at no cost. Landsat is equipped with specific instruments for multispectral remote sensing and has sensors that are useful for UHI characterization and analysis (Ezimand, Chahardoli, Azadbakht, & Matkan, 2021).

This stage consisted of searching for and processing satellite images offered by free USGS platforms. The images were characterized by the variety of bands that they are made up of and have a resolution between 15 and 30 m per pixel.

As the study period covered 2000 to 2020, Landsat 7 Enhanced Thematic Mapper (ETM+) (2000-2013) and Landsat 8 Operational Land Imager (OLI) (2013-2020) images were used. Through a year-by-year search, satellite images were selected from December to March, corresponding to the dry season. Furthermore, images with high cloudiness in the study area were discarded.

Based on the above criteria, the images that met the required conditions were selected (see Table 1). The climatic phenomena present each year were considered since they could have influenced UHI intensity. The El Niño phenomenon can generate temperature increases in contrast to the La Niña phenomenon. The "Neutral" condition in Table 1 indicates that neither of the two climatic phenomena occurred.

Table 1. Satellites, image date used and atmospheric phenomenon for each year studied.

Year	Month	Day	Atmospheric phenomenon	Satellite	Source
2000	Feb	20	Niña	Landsat 7 ETM +	https://eos.com/landviewer/?lat=4.64930&lng=-74.06170&z=11&datasets=2
2002	Feb	25	Neutral		
2003	Jan	27	Niño		
2004	Feb	15	Neutral		
2007	Feb	7	Neutral		
2009	Dec	29	Niño		

Year	Month	Day	Atmospheric phenomenon	Satellite	Source
2012	Feb	21	Niña		
2014	Feb	2	Neutral	Landsat 8 OLI	https://search.remotepixel.ca/#3/16.69/-48.33
2015	Feb	21	Niño		
2018	March	17	Niña		
2020	March	22	Niño		

Given the local atmospheric conditions, lighting, and cloudiness present during data acquisition, the images were subjected to radiometric and atmospheric correction. As such, a radiometric correction was applied to the images via the FLAASH method, using the ENVI Program Version 5.3, in order to manipulate the pixel values and obtain the most homogeneous intensity values, and even correct errors in the pixels. In a complementary manner, an atmospheric correction was performed to reduce the effect of aerosols, as well as the radiance introduced to the sensor reflected in the image (Aguilar, Mora, & Vargas, 2014). Due to sensor failure causing information losses in certain sections of the images, a gap fill correction was carried out on different Landsat 7 EMT+ images (2009 and 2012) through a simple triangulation method.

Socio-economic factors

Several studies have found that UHIs are caused by the convergence of multiple factors, including: population density, economic growth, changing morphology of cities, increased amounts of buildings and impervious surfaces, type of construction materials used, greater vehicular traffic, excessive energy consumption, air pollution, and poor air circulation (Carpio et al., 2020; Grover & Singh, 2015; Litardo et al., 2020; Rizwan et al., 2008). Socio-economic factors were addressed given the degradation of natural resources.

Population increase is a variable that leads to substantial changes in the Spatio-temporal variation of land use and contributes to the loss of water bodies and green areas (Barreto-Martin, Ronal, Calderon-Rivera, Angela, & Mesa-Fernández, 2021). Additionally, anthropogenic heat release can be related to the population and its per capita energy use; the pattern of energy use impacts the heat generated by anthropogenic sources. Previous studies have shown the association between population growth, energy consumption, and UHIs (Grover & Singh, 2015; Oke, 1988;

Rizwan et al., 2008).

Analyzing population density provides an understanding of the environmental impact existing in a city or territory. This variable can be used to measure the magnitude of anthropogenic heat. According to (Ramírez-Aguilar & Lucas Souza, 2019), densities higher than 14,500 inhabitants/km^2 can generate temperatures greater than 1°C, which can lead to higher energy demand, increased thermal energy storage in urban systems, and can aggravate the UHI phenomenon to the point of producing positive feedback loops (Gunawardena, Kershaw, & Steemers, 2019; Yao et al., 2021). Moreover, this situation leads to an increase in the energy consumption requirements of industrial and commercial equipment to maintain their thermal balance to operate (Gaudencio, Ramos Niembro Fiscal Escalante, Maqueda Zamora, Sada Gámiz, & Horacio, 1999; Kao, J Y; Kelley, 1996). Given that Kennedy is the second most populated locality, population and energy consumption patterns were considered variables of interest for the analysis.

Due to limitations regarding access to information for micro-territories such as the study area, it was not possible to establish socio-economic information at the spatial level with the characteristics of the environmental factors. To overcome these limitations, census data and information published by government entities were reviewed. In this manner, it was possible to demonstrate changes by ZPU over the years with respect to population density and energy consumption. These two factors influence urban growth processes, which put pressure on environmental components and urbanization.

2.2.2 Calculation of spectral indices

Once the satellite images were processed, the spectral indices were calculated through operations with the images' bands using the ArcGIS software 10.8.1. The NDVI, NDBI, MNDWI, and NDISI have been used in UHI studies (Chen X. L., Zhao H.M., Li P.X, & Yin Z, 2006; Grigoraș & Urițescu, 2019; Kikon, Singh, Singh, & Vyas, 2016; Min, Lin, Duan, Jin, & Zhang,

276 2019). Furthermore, they have shown significant correlations between LST, built-up areas and
277 vegetation (Kaur & Pandey, 2022). The LST functions as a parameter to control the water and
278 energy balance between the atmosphere and the land surface. Table 2 describes the equations used
279 to calculate the spectral indices.

280 Table 2. Spectral indices for environmental factors

Index	Equation	References
Normalized difference vegetation index enables an estimation of the quantity and quality of vegetation based on the portion of red light absorbed and the near infrared reflected. The index ranges from -1 to 1, in which negative values correspond to water surfaces, rocks, or artificial structures and positive values represent vegetation.	$NDVI = \frac{NIR - RED}{NIR + RED}$ (1)	(Grigoraș & Urițescu, 2019; Madanian, Soffianian, Soltani Koupai, Pourmanafi, & Momeni, 2018; Yuan & Bauer, 2007)
Normalized difference built-up index enables the identification and estimate of built or under construction areas. It also facilitates the analysis of urban growth and built-up areas. The index values range from -1 to 1; negative results indicate the presence of vegetation, and positive values correspond to built-up areas or anthropogenic infrastructures.	$NDBI = \frac{SWIR - NIR}{SWIR + NIR}$ (2)	(Musse, Barona, & Santana Rodriguez, 2018; Zha, Gao, & Ni, 2003)
Modified normalized difference water index enables the recognition of water covers, isolating them from other coverings. Its range is -1 to 1; the positive values are interpreted as water; and values close to zero or negative indicate vegetation or soil.	$MNDWI = \frac{GREEN - SWIR}{GREEN + SWIR}$ (4)	(X. Chen & Zhang, 2017; Xu, 2006)
Normalized difference impervious surface index (NDISI): this index has been used to extract impervious surfaces. NDISI removes noise such as soil and water. The surface radiation is maximized by using the thermal wavelength (TIR), minimizing the reflectance of NIR, SWIR, and GREEN per impermeable surface. Positive values represent impermeable surfaces, as opposed to negative values.	$\text{NDISI} = \frac{TIR - \frac{(GREEN+NIR+SWIR)}{3}}{TIR + \frac{(GREEN+NIR+SWIR)}{3}}$ (5)	(Estoque and Murayama, 2015; Musse et al., 2018; Xu, 2010)

281

In which, NIR is near infrared, RED is the red band, SWIR is short-wave infrared 1, which differentiates soil and vegetation moisture; this wave penetrates through thin clouds. GREEN corresponds to the green band. For Landsat 7, these bands are 4, 3, 5, and 2; and for Landsat 8, they are 5, 4, 6, and 3.

2.2.3 Calculating Land Surface Temperature (LST)

Reflectance, brightness, and surface emissivity were calculated by processing the bands that store digital thermal information in each of the selected scenes (see Table 1). The results of this calculation enable the identification of the LST spatial distribution pattern.

The images' thermal bands, band 6 for Landsat 7 and band 10 for Landsat 8, were used to calculate LST. Using the method proposed by USGS (Ihlen & USGS, 2019b, 2019a) and through equations (6) and (7), a conversion of the digital number to a radiometric scale was performed.

For Landsat 7,

$$L\lambda = \left(\frac{LMAX_\lambda - LMIN_\lambda}{QCALMAX - QCALMIN}\right) * (QCAL - QCALMIN) + LMIN_\lambda \quad (6)$$

In which $L\lambda$ is the reflectance of the top of the atmosphere (TOA) in $\frac{W}{m^2 * sr * \mu m}$; $LMAX_\lambda$ and $LMIN_\lambda$ are radiance values obtained from image metadata; QCAL is the quantified pixel value calibrated in a digital number; QCALMAX and QCALMIN are the maximum and minimum pixel of band 6. The images' digital numbers were transformed into radiation units.

For Landsat 8,

$$L\lambda = M_L * \text{QCAL} + A_L \quad (7)$$

In which $L\lambda$ is TOA in $\frac{W}{m^2 * sr * \mu m}$; M_L is the multiplicative brightness scale factor for band 10; A_L is the additive radiance scale factor for the same band; and QCAL is the quantified value of the digitally calibrated pixel.

The brightness temperature (TB) was then calculated using equation (8), which enables the irradiation to be transformed into surface temperature in degrees Kelvin (Ihlen & USGS, 2019a,

2019b).

$$TB = \frac{K_2}{ln\left(\frac{K_1}{L\lambda}+1\right)} \quad (8)$$

In which K_1 and K_2 are calibration constants taken from the image metadata. Lastly, the LST is calculated via equation (9); the results are presented in degrees Kelvin.

$$LST = \frac{TB}{1+\left[\lambda*\frac{TB}{a}\varepsilon\right]} \quad (9)$$

In which λ is the wavelength of the radiance emitted; a is $1.438x10^{-2}$ mK (Estoque & Murayama, 2017; Senanayake et al., 2013) and ε is the surface emissivity, which is calculated by equation (10) (Grigoraș & Urițescu, 2019; Wang, Ma, Ding, & Liang, 2018).

$$\varepsilon = 0.004 * Pv + 0.986 \quad (10)$$

In which Pv is the vegetation proportion calculated as shown in equation below (11):

$$Pv = \left[\frac{(NDVI - NDVI_{min})}{(NDVI_{max} - NDVI_{min})}\right]^2 \quad (11)$$

A raster file showing the spatial distribution of the LST for each pixel was obtained from equation 9. These values ranged from the lowest to the highest temperatures and were classified via equivalent intervals. This univariate classification method divides the data into *n* categories or classes with the same range or amplitude value (de Smith, Goodchild, Longley, & Associates, 2021). This makes it possible to see relative temperature values with respect to other values obtained for the study area. In this research study, ten classes with amplitude intervals of 3 degrees were established. As such, this classification facilitated the comparison of the temperatures' variability in the years studied, as well as the identification of relevant UHI points in each of the micro-territories.

2.2.4 Analysis of the UHI phenomenon

The information generated in the previous stage made it possible to perform an LST

distribution analysis. To better understand UHI behavior, distance vs. temperature profiles were made in four different directions: 1) north-south, 2) northwest-southeast, 3) west-east, and 4) northeast-southwest; with the pixel value determined every 500 meters. The year-by-year results were categorized by the dominant climate phenomenon (El Niño or La Niña in each case) and based on these profiles, the micro-territories with the highest or lowest temperatures in the locality were identified.

2.2.5 Analysis of the relationship between variables and UHI

Urban sustainability is primarily related to the behavior of the environmental, social, and economic dimensions; in which urban growth generates a series of pressure points that can be seen in these dimensions' behavior.

A principal component analysis (PCA) was performed to identify the degree of relationship between variables. In addition to reducing the set of variables to their linear combination in principal components, this method extracts important information from the analyzed variables. The PCA also makes it possible to identify the contribution of variables (environmental and socio-economic factors) and individuals (each point in the micro-territory) to the main components. In other words, it was possible to identify not only the contribution of the variables analyzed to the manifestation of the UHI phenomenon, the PCA also facilitated the identification of the specific contribution of each micro-territory (ZPU) to the UHI phenomenon at the spatial level.

The input information consisted of a band composition from the raster images of the spectral indices presented in Table 2, along with the population density and energy consumption variables. The band composition was performed with the ArcGIS software 10.8.1, followed by the PCA analysis carried out with the free access software R.

3 Results

3.1 Environmental factors

Rapid urbanization has affected the natural environment of urban areas. Consequently, the UHI phenomenon occurs, which are created and intensified by the increase of impermeable surfaces or heat produced by human activities, as well as by the reduction of green spaces in a territory. In this vein, vegetation dynamics, the expansion of built-upon soil, and water bodies are environmental factors that can influence the formation and behavior of UHI. Therefore, using spectral indexes facilitated the calculation and analysis of these variables and their correlation with LST, as affirmed by (Ezimand, Kakroodi, & Kiavarz, 2018; Kaur & Pandey, 2022).

3.1.1 Vegetation dynamics

Vegetation dynamics were analyzed based on the NDVI from 2000 to 2020 (see Fig.3). Most of the green area was located to the north of the locality. In 2000, about 36% of the study area (13.98 km^2) corresponded to a zone with vegetation. A notable reduction in vegetation has occurred since 2003, primarily attributed to the increase in building construction in the area.

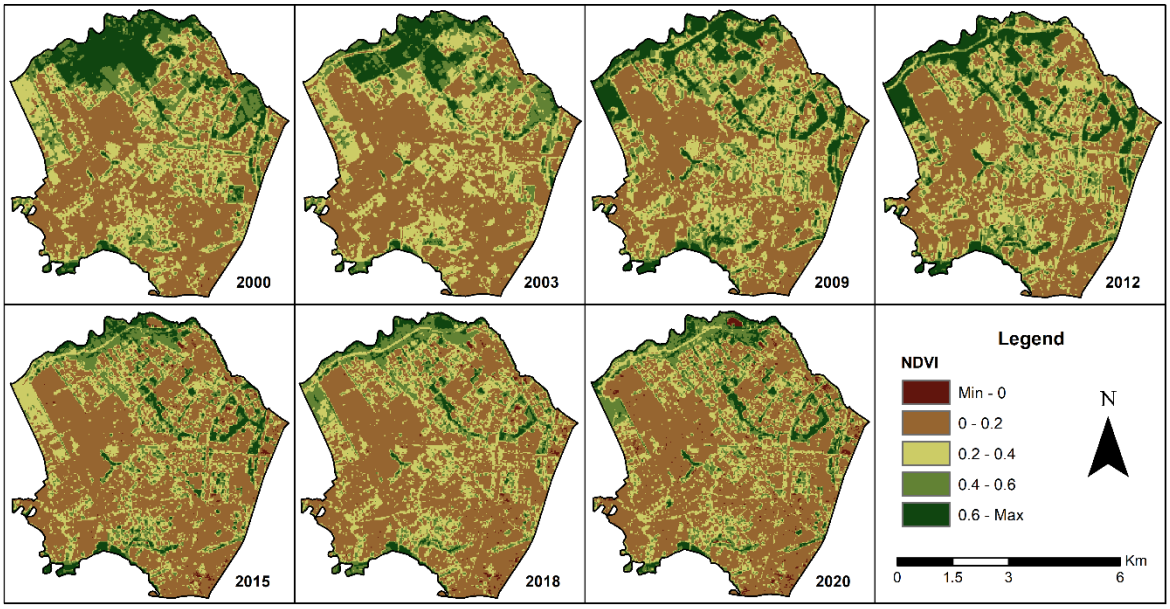

Fig. 3. Dynamics of the Normalized Difference Vegetation Index

By 2009, vegetation had been reduced by 9.62 km^2, and the first consolidation of buildings in the northern zone can be detected. In 2020, there are approximately 7.14 km^2 of vegetation areas, which fall in the NDVI range of 0.2 to values > 0.6 (see Fig.3). The range between 0.2 and 0.4 corresponds to areas with scarce or dispersed vegetation; between 0.4 and 0.6 corresponds to areas with moderate vegetation; and NDVI values greater than 0.6 represent locations where the density of vegetation is most likely green and healthy.

3.1.2 Built-up areas and impervious surfaces

Kennedy is mostly covered by buildings and impermeable surfaces such as roads and sidewalks with scarce vegetation. The behavior of bare soils or built-up covers is inverse to that of the vegetation (see Fig.4). In 2000, the area with buildings was approximately 22.1 km^2, which were consolidated in the southern part of the locality. Seven years later, the area with buildings increased to 26.9 km^2, reaching 28.3 km^2 in 2020. In the first years of the study, land occupancy for housing in illegal urbanizations continued in areas such as the La Vaca Wetland (in the Corabastos ZPU), in the northern part of the locality in areas of El Tintal, particularly on the banks of the Bogotá River, northwest of Kennedy (Escobar Franco, 2012). The greatest variations occurred in the northern part of the locality.

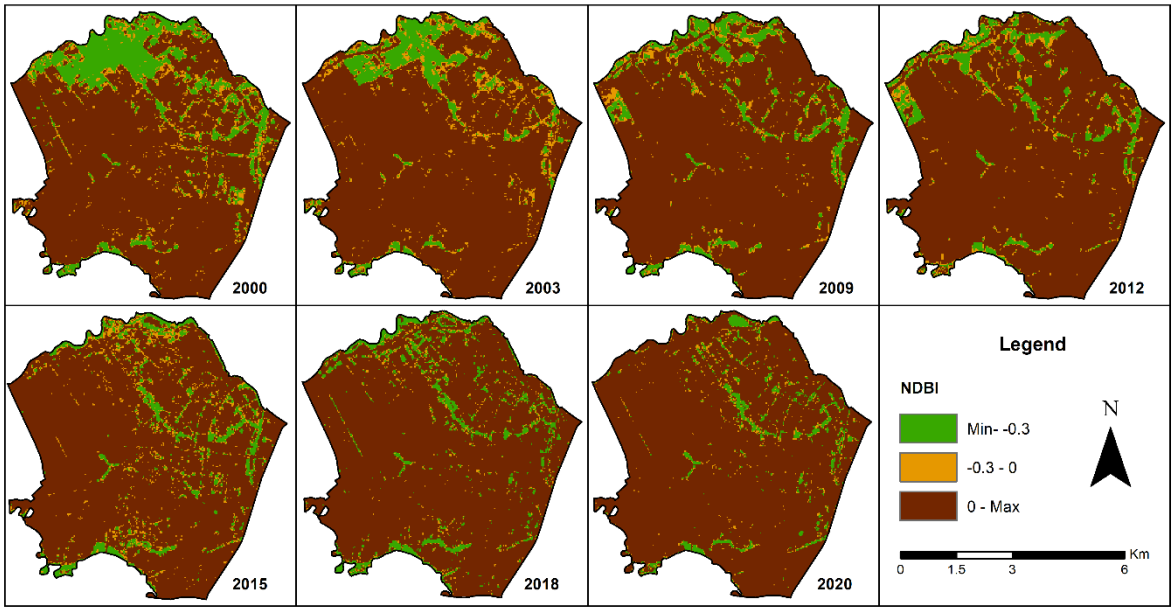

Fig. 4. Dynamics of the Normalized Differential Build-up Index

3.1.3 Bodies of water

The bodies of water were evaluated by measuring the MNDWI. Figure 5 shows the years in which changes occurred. In 2000, Lake Timiza, which previously could not be seen, stood out in the southern area. In the following years, there were no variations in the MNDWI. However, based on the spatial operations with geographic information of the city, a reduction of the water mirrors was identified, from 0.032km^2 in 2000 to 0.0154 km^2 in 2014. This reduction occurred in the wetlands located in the center and north of the locality.

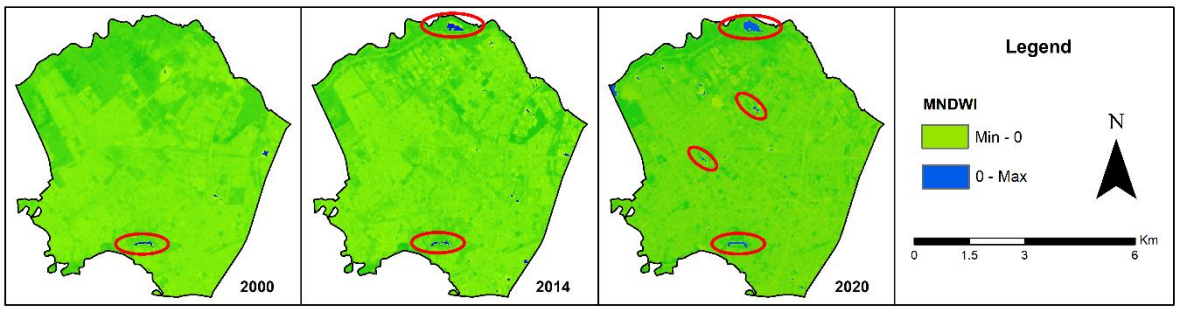

Fig. 5 Bodies of water

It is possible that the reduction in vegetation recorded over the years may have revealed the bodies of water. Grasslands also reduced from 0.895 km^2 in 2000 to 0.263 km^2 in 2014. For this reason, as of 2014, the Pondaje Lagoon, created to regulate the flow of water and prevent flooding in the area, is seen in the northern part of the locality. By 2020, the El Burro and La Vaca wetlands in the center of the locality can be seen to a lesser extent.

3.2 Socio-economic factors

The socio-economic factors analyzed correspond to changes in population density and energy consumption flows, which are integral components of the development of urban spaces. The larger the population, the greater the pressure on resources, and the greater the energy requirements. Sustainable cities and communities entail balancing pressure generated to guarantee the residents' well-being and quality of life, as they are committed to providing adequate housing, access to transport systems, increased inclusive and sustainable urbanization. The above is in addition to

safeguarding the area's natural heritage, reducing environmental impacts, and universal access to green areas (UNDP, 2020). These challenges are intensifying for urban areas such as Kennedy. The dynamics of local population density and energy consumption are analyzed below.

3.2.1 Population density

Population density maps were created based on census data (SDP, 2020) (see Fig.6). In 2005, the average population density of the locality was 24,625 inhabitants/km^2, ranging from 3,800 to 50,500 inhabitants/km^2. Patio Bonito was the most densely populated ZPU in the city, exceeding the gross density of Bogotá. In recent years, population density figures have exceeded those in other cities in Latin America such as Quito, Ecuador (5401 inhabitants/km^2) and Mexico City, Mexico (5966 inhabitants/km^2).

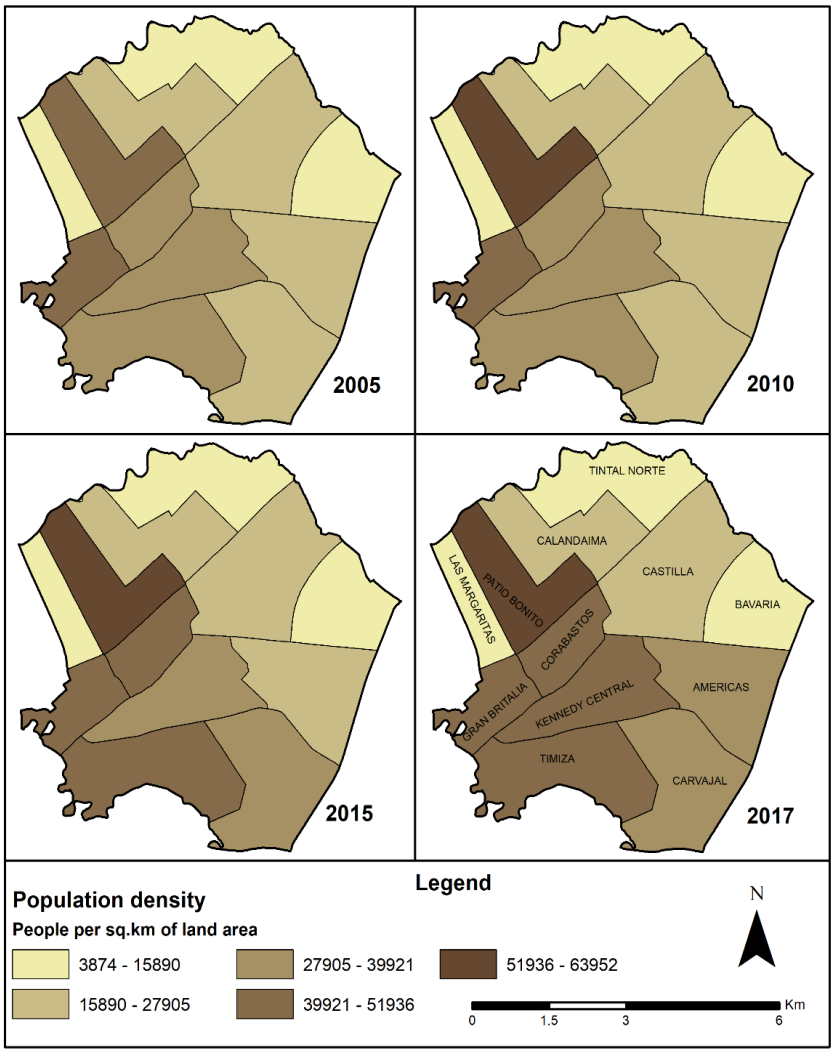

Fig. 6. Population density by ZPU in Kennedy

An increase in population density over the years can be seen in the central zone and south of the locality in the ZPUs of Corabastos, Kennedy Central, Timiza, Carvajal, and Américas.

3.2.2 Energy consumption

Kennedy is one of the localities of Bogota with the highest concentrations of electric energy consumption (Alcaldía Mayor de Bogotá, 2017). Over the years, there has been a progressive increase in the consumption of energy for residential, commercial, and industrial use (see Fig.7). However, in the eastern part of the locality, industrial consumption has decreased, while residential and commercial consumption have increased. The ZPUs of Patio Bonito, Timiza, and Castilla are

the areas with the highest residential energy consumption; Carvajal has the highest consumption for commercial and industrial use.

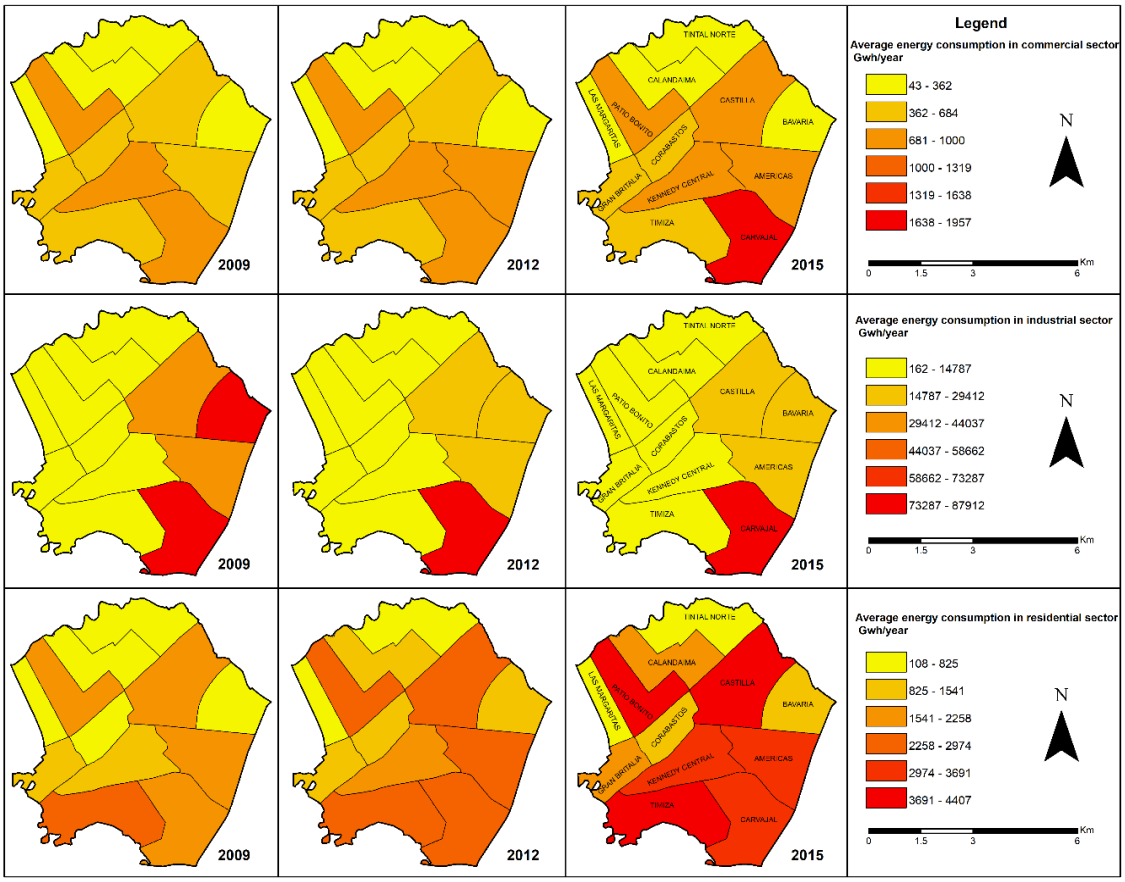

Fig. 7. Dynamic of the energy consumption in Kennedy

3.3 LST spatial-temporal pattern

The LST distribution was classified in ranges of 3ºC (see Fig.8). The lowest temperatures occurred in 2000 in the north of the locality due to the presence of healthy consolidated vegetation. Two years later, temperatures increased in the eastern and southern parts of the locality, ranging from 28° to 33ºC. The LST distribution was more uniform throughout the area with values between 12° and 33°C during the following year. However, small areas in the center of the locality stand out, such as the ZPUs of Corabastos and Kennedy Central, where temperatures are higher than 28ºC. This pattern is seen in every year, and from 2012 its increase exceeds 5° Celsius.

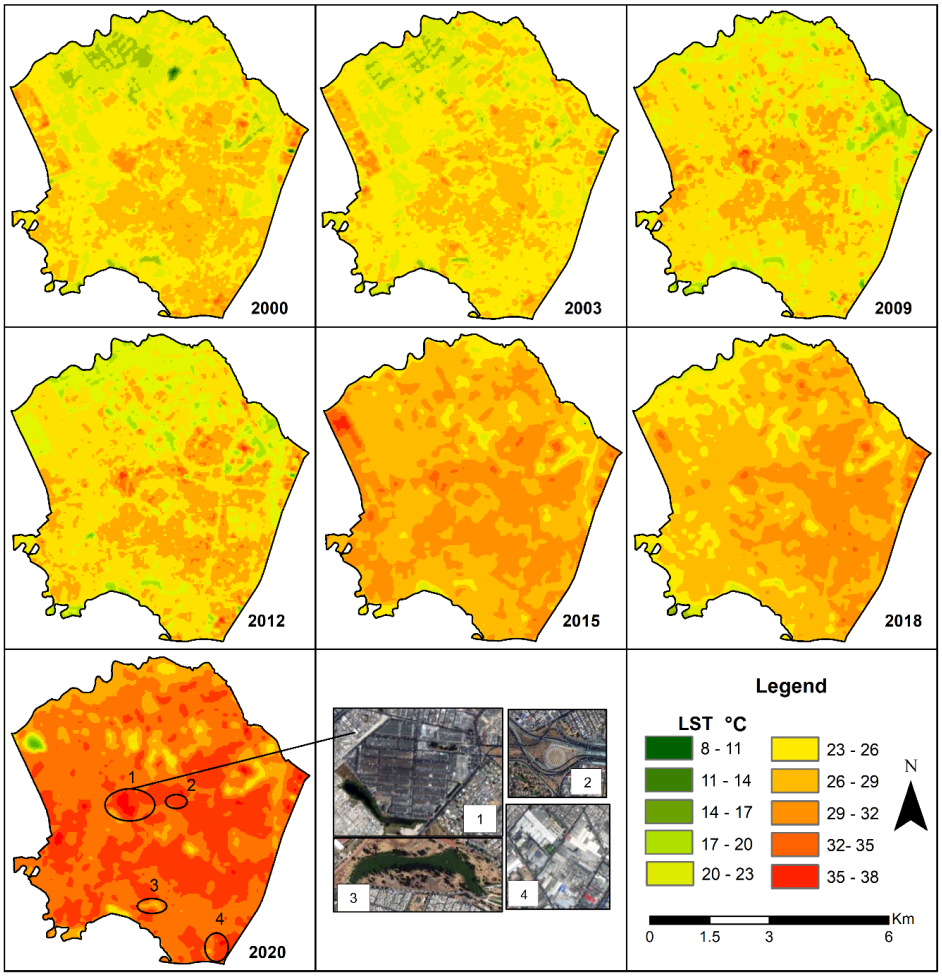

Fig. 8 Land surface temperature dynamic

Over the 20 years analyzed, impervious built-up areas (principally buildings, roads, and public space infrastructure) grew by approximately 6.2 km^2. This led to increased temperatures that exceeded 5°C in the northern zone of the locality, particularly in the Patio Bonito, Calandaima, and Tintal Norte ZPUs. Moreover, the amount of green areas decreased; whose temperatures are characterized by being the lowest and most conformable in the territory (8-14°C). In the areas where urban expansion began, temperatures started to rise due to changes in impermeable surfaces that favor the absorption of radiation and the emission of heat into the environment.

These results were contrasted with the locality's economic and urban conditions. The area with the highest temperatures coincides with the location of the country's main supply center; Corabastos (image 1 in Figure 8). Approximately 1,200 vehicles carrying supplies enter the area

every day, most of which are older models, which emit atmospheric pollutants. Temperature increases cause an accelerated production of smog, concentration of pollutants, and impacts on local meteorology (Ngarambe, Joen, Han, & Yun, 2021), which cause PM_{10} to exceed WHO recommendations (WHO, 2006). The increase in residential and commercial energy consumption in the south and east of the locality also contributes to this process (see Fig.7).

Since 2012, there has been a homogeneity of temperature distribution changes, with approximately half of the locality having temperatures between 26º and 33º Celsius in the same south-east area. In 2015, temperatures intensified in most of the territory due to the presence of the El Niño phenomenon, while in 2018, temperatures decreased, which can be attributed to the precipitation generated by the La Niña phenomenon. In 2020, the LST was greater than 26ºC throughout most of the locality, with a maximum of 38ºC, which also coincides with the ZPUs with high energy consumption for the different analyzed uses (see Fig.7).

As Kennedy is a locality with low levels of vegetation (3584 trees/km^2 in 2020) compared to built-up areas, it is vulnerable to continue experiencing the intensity of UHIs. In certain micro-territories, there has been uncontrolled urbanization, mainly in peri-urban areas, which has affected land use and increased urban expansion in natural areas (Dobbs et al., 2018). This contrasts the fact that 25% of urban areas are unplanned or informally planned at the global level (UN-Habitat, 2019).

The LST behavior was analyzed by profiles (see Fig.9), in which the locations with the highest temperatures in the micro-territories were highlighted. The blue lines represent the years in which the La Niña phenomenon occurred, the red lines represent the El Niño phenomenon, and the green lines indicate the neutral years. Figure 9 with a north-south heading, shows the extreme low temperature values, and a peak in the center of the locality, where a mass public transport station is located (Banderas Station, Image 2 in Figure 8). At this site, the highest temperatures were reached, surpassing 33ºC in 2018.

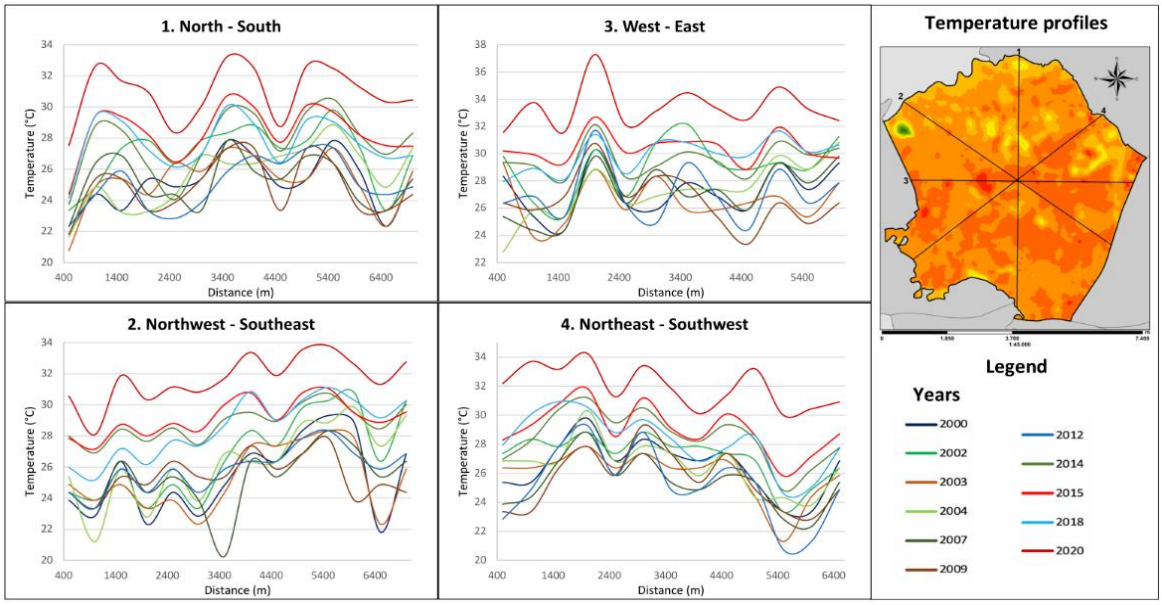

Fig. 9. Land surface temperature profiles

Despite most of the curves showing a uniform behavior in years in which the El Niño phenomenon was present (see the red curves in Fig.9), the behavior is above the others. The graphs show a similar behavior between 2015 and 2020, but in 2020 the temperature increased by approximately 2ºC when compared to 2015.

In the west-east direction, there is a temperature increase in the first 1500 meters, coinciding with the central supply center which consists of a consolidated built area of 420,000 m^2. This area is known for its economic activity and daily vehicle movement. Moreover, the average building height is 5 – 6 floors per block in this location, which can hinder proper air circulation.

It is important to mention that there is a noteworthy pattern of temperature decreases linked to bodies of water. Nevertheless, in the 20 years analyzed, the temperature rose by approximately 3.6ºC, an annually progressive increase. This rise means that minimum temperatures are mostly above 14ºC and maximum temperatures average 34.7º, with the highest temperature in 2020 being 37.84º Celsius. There was an increase in the years when El Niño occurred; however, it did not change the trends in LST behavior.

Studies in the global context mostly analyze areas larger than 100 km^2 and none have focused on local areas, or micro-territories. When analyzing UHI behavior by profile, as was the

case in the study developed by Estoque and Murayama (2017), the UHI pattern in Kennedy largely held steady during the final years of the study from 2015 to 2020. The first years of the study had low temperature values, as there was a greater presence of vegetation (average temperature of 22.5ºC during 2000-2003).

3.4 Relations between UHI and impact factors

The loss of vegetation coverage has resulted in an increase of UHI in the locality, as the amount of vegetation influences the LST via the heat flow from the surface through evapotranspiration. Furthermore, trees provide shade and cooling that can prevent direct exposure of land surfaces to solar radiation (Singh et al., 2017; Soltani & Sharifi, 2017).

The PCA analysis made it possible to establish three components (see Fig. 10 and Table 3) that account for 73% of the variance in the data. The first component: Dim 1 (37.7% of the variance), highlights central elements of urban expansion. The variables with the greatest contribution (67%) in this component were NDVI, NDBI, MNDWI, and commercial energy consumption with correlations greater than 70% with Dim 1 (see Fig. 10a and Table 3). Although weak, there is also a positive correlation between population density (PD) (55%), residential energy consumption (REC) (53%), industrial energy consumption (IEC) (50%), and LST (49%), which are elements that characterize the effects of urban growth (see Table 3). As in the study developed by Chen and Zhang (2017), the relationship between LST and NDBI had one of the strongest linear positive correlations, which can be attributed to the heterogeneity of the land surface, particularly in areas with little vegetation. The relationship between LST, and NDBI is linearly positive, given that when built-up areas or soils without vegetation increase, temperature is not absorbed or regulated, which generates an increase of temperatures in urban centers.

The second component, Dim 2, correlates energy consumption in the different analyzed uses (19.9% of the variance) with a 56.6% contribution to this component. The relationship between

the first and second components is shown in Fig. 10a. Dim 1-Dim 2, which shows both the quality of the variables and their correlation with the components (see Table 3).

In the clusters, it is also noted that LST and NDVI have a moderate negative correlation (-0.67), given that lower temperatures occur in areas with dense vegetation. NDVI also has an inverse correlation with NDBI (-0.95). Greater urban growth and less vegetation are correlated with UHI intensity (see Figure 10b and Table 3).

The third component, Dim 3, called LST, accounts for 15.3% of the variance in the data and includes population density variables, energy consumption by residential and industrial users, the NDISI, and LST, which are the variables that contribute the most to this component (94.2%). Figures 10b Dim 2 – Dim 3 and 10c Dim 1 – Dim 3 show the relationship of this component with Dim 1 and 2. In each case, the correlation of the variables with each component is evident by the fact that they are close to the edge of the circumference (see Figure 10c and Table 3).

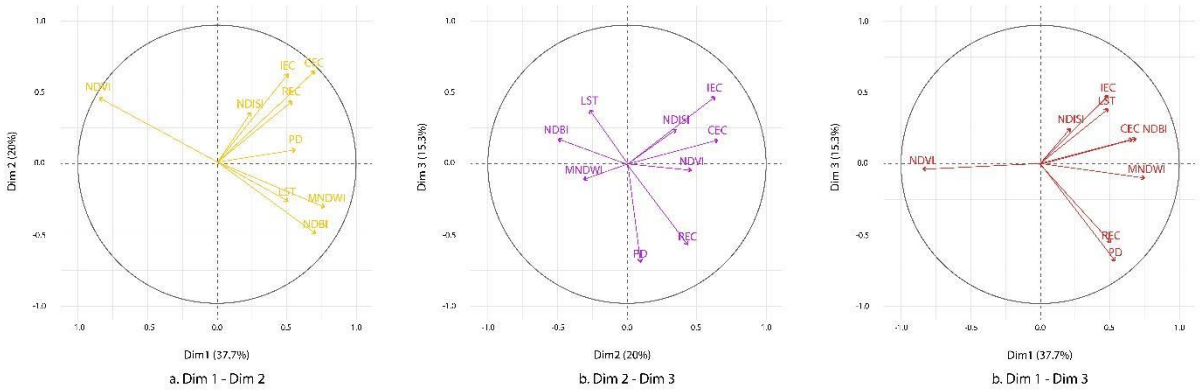

Fig. 10. Principal component analysis

In its development, the PCA included the following elements: vegetation variation represented in the NDVI index, variation of built-up areas represented in the NDBI index, variation of water bodies and wetlands represented in the MNDWI index, impervious surfaces variation represented in the NDSI index, population density (PD), commercial energy consumption (CEC), industrial energy consumption (IEC), residential energy consumption (REC), as well as land surface temperature (LST).

Table 3. Principal components and variable correlation

Variable	Dim.1 (Urban expansion)	Dim.2 (Energy consumption)	Dim.3 (LST)
LST	0,49	-0,27	0,39
NDVI	-0,85	0,46	-0,04
NDBI	0,70	-0,51	0,19
MNDWI	0,76	-0,32	-0,11
NDISI	0,23	0,35	0,26
PD	0,55	0,09	-0,71
REC	0,53	0,44	-0,58
IEC	0,50	0,63	0,48
CEC	0,69	0,65	0,18

These analyses can also be used to compare dimensions and identify the micro-territories that contribute the most to the components (see Fig.11). As such, the largest contributions were found in the ZPUs of Patio Bonito, Carvajal, and Tintal Norte, which coincide with the areas with the highest population densities, elevated energy consumption, growth in built-up areas, and reduction in green areas.

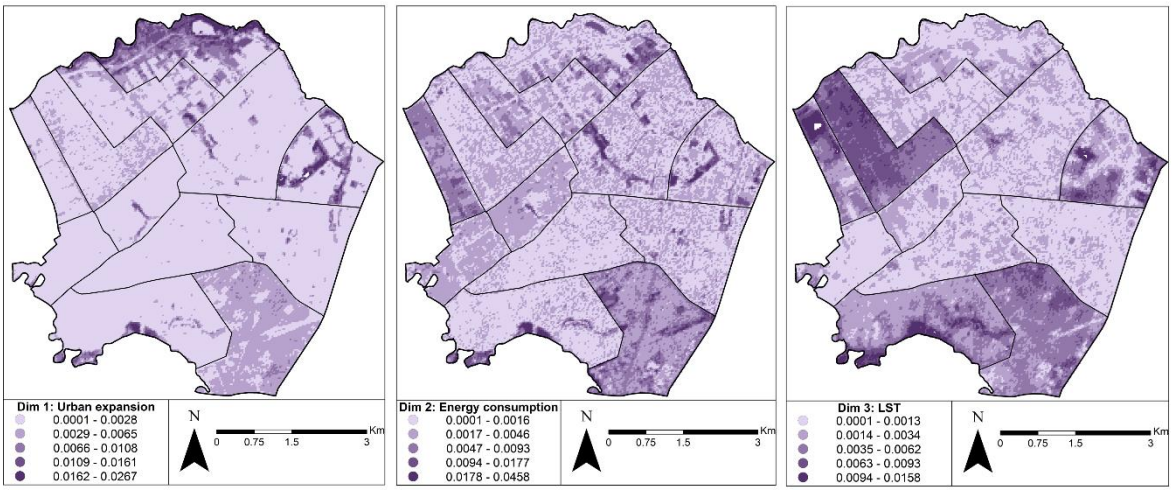

Fig. 11 Contribution from micro-territories to the components

Figure 11 highlights the contributions from the north and east of the locality to urban expansion. North and south Kennedy contribute more to energy consumption (Dim 2). The territories that contribute to component 3 (see Fig.11 Dim 3: LST) are mainly located in the south and west of Kennedy. A mix of commercial, residential, and industrial activities is characteristic in those areas (Patio Bonito, Timiza, and Carvajal ZPUs). The above once again demonstrates the

572 implications of urban growth on urban sustainability conditions.

573

574 **4 Discussion**

575 *4.1 Influence of urban growth on the UHI phenomenon*

576 This study identified the behavior of urban growth based on the environmental and socio-
577 economic factors analyzed, thus determining their influence on the generation of UHIs.

578 Regarding environmental factors, changes in land cover play an important role in the
579 development of UHIs. Vegetation decreased by 48.6% over the last 20 years, which was replaced
580 by impermeable surfaces and consequently led to greater deterioration of environmental quality.
581 These finding are consistent with the results from studies carried out by (Ezimand et al., 2018;
582 Portela et al., 2020; Yue, Liu, & Fan, 2012; Zhang, Estoque, & Murayama, 2017), thus reaffirming
583 the importance of environmental factors such as vegetation and the presence of water surfaces in
584 mitigating the UHI phenomenon. This is further supported by the results of the PCA, which found
585 that three components (urban expansion, energy consumption, and LST), had an overall
586 contribution of 73% to the variance of the data. The greatest contribution was found among the
587 environmental variables, NDVI, NDBI, and MNDWI.

588 According to the energy balance theory, as affirmed by Yue et al., (2012), UHIs are created
589 by an increase of impervious surfaces, reduced vegetation, and the discharge of anthropogenic heat
590 from energy consumption. This study found that in addition to the strong influence of the above
591 variables, energy consumption is prominent in commercial areas coinciding with areas with higher
592 LSTs, where the anthropogenic heat release primarily from vehicle emission sources corresponds
593 with the elements defined by Yue et al., (2012).

594 This study also reaffirmed the findings of Yue et al., (2012), regarding the value of using
595 PCA to identify the primary components that contribute to the formation of UHIs. In this case, three
596 components had values greater than 70% in contributing to the data's variability.

597 Additionally, developing a PCA made it possible to determine the micro-territories that

most contribute to this phenomenon in the study area, namely the ZPUs of Patio Bonito, Carvajal, and Tintal Norte.

It is important to consider population growth trends; as population increases result in a greater demand for resources such as water, energy, and soil. As Kennedy does not have new zones for construction, lower buildings will inevitably be replaced by higher ones to house a larger population. This process changes the morphology of the land and causes air quality and temperature changes. The above is comparable with the results found by (Bokaie et al., 2016; Parvez M.I., 2019), and is reflected in this study in the analysis of environmental and socio-economic indices, as well as the PCA. This situation will require measures to be adopted to balance temperatures. For example, these could include green belts in different areas, particularly those that contribute the most to components 1 (urban expansion) and 3 (LST), according to PCA those micro-territories were the ZPUs Tintal Norte, Patio Bonito, Timiza, and Carvajal.

The formation of UHI occurs mainly in the center of the locality (Corabastos and Kennedy Central ZPUs), as it is the area with the highest vehicle mobility and consolidated residential and commercial areas. These findings are similar to other studies, such as the one developed by Amanollahi et al. (2016), which presented the critical points of UHI in parts of the city with commercial and residential areas, main roads, and even in areas for agricultural use. In Kennedy, LST progressively increased, with a notable homogenization of the temperature over the entire locality for the last years of the study. This situation shows the relevance in extending the resolution of spatial analysis, since the behavior of UHI reflected by the ZPU in Kennedy as a territory within a large city behaves similarly in capital cities.

In this study, activities related to population density were added, which include greater vehicle traffic entering urbanized areas and the operation of commercial areas with their corresponding energy consumption such as ZPUs Carvajal, Corabastos, Kennedy Central, and Patio Bonito. These results are comparable with the study developed for Bogotá by Ramírez-Aguilar and Lucas (2019) demonstrating the relationship between population density and heat intensity.

Moreover, according to (Zhang, Estoque, & Murayama, 2017), there is an indirect relationship between those factors, since population density is a driver of different land uses and economic activities.

The procedure developed in this research study can be applied to several urban areas to identify the territories that contribute the most to the UHI phenomenon, in addition to the most appropriate urban and landscape planning measures. It is also applicable to cities such as Ghaziabad (India); one of the most polluted cities in the world with a population density comparable to some of the ZPUs in Kennedy, as well as Orangi Town in Karachi (Pakistan) and Neza (Mexico).

4.2 Implications of UHI on urban sustainability

Urban areas face major challenges in terms of sustainability, as they must balance the demand for resources inherent to urban growth with existing ecosystems. Consequently, it is necessary to not only establish measures to mitigate local pollutants from mobile and stationary sources, but to also create sustainable micro-territories including buffer zones for environmental aspects. Future research should correspond to establishing measures and analyzing correlation with reducing the causes of UHI in each micro-territory analyzed in this study.

The approach outlined in this research study contributes to establishing specific measures regarding urban landscape design and its potential to mitigate UHIs and local pollutants, as was examined by Rizwan et al., (2008). Given the difficulty of creating green areas in densely populated areas, one way to mitigate the effects of UHIs in Kennedy is to improve its vegetation cover, either on roofs and green walls or by restructuring buildings to increase the number of trees in the area, as was identified by Litardo et al., (2020). Other measures include adopting energy efficiency policies to reduce unintentional heat-generating emissions in urban areas, which can contribute at the micro-territorial level, in addition to implementing measures at a larger scale. For their part, urban and landscape planning processes require using new elements, such as different materials in buildings and infrastructures that reflect radiation and enable an LST balance to be maintained.

5 Conclusions

This study used a combination of tools (spectral indexes, census information, principal component analysis) to analyze from the micro-territorial level, the influence of urban growth on the UHI phenomenon over the last two decades (2000-2020) in the locality of Kennedy, in Bogotá, Colombia. Using this combination of tools made it possible to determine the environmental and economic factors that most contribute to the formation of UHIs.

The most representative variables for the formation of UHIs were the reduction of vegetation, more built-up areas, and fewer bodies of water. The micro-territories that contributed the most to this phenomenon are located where anthropogenic activities are developed, coupled with changes in the vegetation cover, namely: Patio Bonito, Carvajal, and Tintal Norte. The PCA revealed an inverse relationship between NDVI and LST, as did the MNDW and NDBI indices. These results indicate that the lower the quality, quantity, and development of vegetation, the higher the LST. Vegetation was reduced by 48.6% in the study area over the last 20 years, which was linked to changes in vegetation cover due to urban growth. For this reason, environmental determinants at the micro-territorial level should promote more urban trees and green areas to mitigate the effects of UHIs in areas with higher concentrations of LST.

Urban areas and the anthropogenic activities that take place in them impact LST variations. This occurs mainly in small territories with high population densities and high energy consumption, such as those analyzed in this study. It is possible that the increase in population density, coupled with the anthropogenic heat generated in the locality, may result in higher energy demand linked to the operation of industrial and commercial equipment required to maintain a temperature equilibrium. Moreover, in the last twenty years, Kennedy, with an urban area of 38.58 km^2, experienced LST increases up to 5°C due to more built-up areas; 28% in the period of analysis.

In this study, the highest temperatures were reflected in places where vehicle traffic entails a combination of public passenger transportation and cargo vehicles. Regarding the population

density, Patio Bonito stood out as the most densely populated ZPU, while the Corabastos, Timiza, Kennedy Central, and Américas ZPUs had relevant changes when compared to 2005. It should be noted that this increase is also reflected in greater residential energy consumption in areas where there was no substantial increase in population density, in addition to the commercial activities and traffic flow that contributed towards greater energy consumption.

A limitation of this study was the specific quantification of anthropogenic heat of the spatial level analyzed. In response, future studies could monitor anthropogenic sources with higher levels of spatial resolution to address this limitation.

This study reflects the importance of implementing mitigation strategies to reduce LTS, due to its rising trend as shown herein. This research study established the procedural approach applicable to tropical micro-territories, the results and analysis of which are comparable with other areas where progress is being made in organizing urban areas. Using this established procedure is a tool to monitor challenges related to sustainable development goals, primarily concerning sustainable cities and communities.

Declarations

Authors' contributions: All authors contributed to the conception and design of the study. Data collection, analysis and interpretation were performed by Nidia Isabel Molina-Gómez, Laura Marcela Varon-Bravo and Ronal Sierra-Parada. Nidia Isabel Molina-Gómez and Laura Marcela Varon-Bravo wrote the original draft; Nidia Isabel Molina-Gómez, Laura Marcela Varon-Bravo, Ronal Sierra-Parada and P. Amparo López-Jiménez wrote, reviewed and edited the final manuscript; and P. Amparo López-Jiménez was involved in supervision. All authors have read and approved the final manuscript.

Funding: No funding was received to assist with the preparation of this manuscript.

Conflict of interest/Competing interests: The authors declare that they have no conflict of

interest.

Availability of data and material: all data and materials support the published claims and comply with field standards.

Code availability: The software application supports the published claims and comply with field standards.

Ethics approval: Not applicable.

Consent to participate: Not applicable.

References

Aguilar, H., Mora, R., & Vargas, C. (2014). Atmospheric Correction Methodology for Aster, Rapideye, Spot 2 and Landsat 8 Images With Envi Flaash Module Software. *Revista Geográfica de América Central*, *2*(53), 39–59. https://doi.org/http://dx.doi.org/10.15359/rgac.2-53.2

Alcaldía Mayor de Bogotá. (2017). *Consumos energéticos urbanos por usos y actividades económicas por UPZ en Bogotá DC 2009-2012-2015*. Bogotá.

Amanollahi, J., Tzanis, C., Ramli, M. F., & Abdullah, A. M. (2016). Urban heat evolution in a tropical area utilizing Landsat imagery. *Atmospheric Research*, *167*, 175–182. https://doi.org/10.1016/j.atmosres.2015.07.019

Barreto-Martin, C., Ronal, S.-P., Calderon-Rivera, D., Angela, J.-L., & Mesa-Fernández, D. (2021). Spatio-temporal analysis of the hydrological response to land cover changes in the sub-basin of the Chicú river, Colombia. *Heliyon*, *7*(March). https://doi.org/10.1016/j.heliyon.2021.e07358

Bokaie, M., Zarkesh, M. K., Arasteh, P. D., & Hosseini, A. (2016). Assessment of Urban Heat Island based on the relationship between land surface temperature and Land Use/ Land Cover in Tehran. *Sustainable Cities and Society*, *23*, 94–104. https://doi.org/10.1016/j.scs.2016.03.009

Carpio, M., González, Á., González, M., & Verichev, K. (2020). Influence of pavements on the urban heat island phenomenon: A scientific evolution analysis. *Energy and Buildings*, *226*, 110379. https://doi.org/10.1016/j.enbuild.2020.110379

Chen, X. L., Zhao, H. M., Li, P. X., & Yin, Z. Y. (2006). Remote sensing image-based analysis of the relationship between urban heat island and land use/cover changes. *Remote Sensing of Environment*, *104*(2), 133–146. https://doi.org/10.1016/j.rse.2005.11.016

Chen, X., & Zhang, Y. (2017). Impacts of urban surface characteristics on spatiotemporal pattern of land surface temperature in Kunming of China. *Sustainable Cities and Society*, *32*, 87–99. https://doi.org/10.1016/j.scs.2017.03.013

de Smith, M. J., Goodchild, M. F., Longley, P. A., & Associates. (2021). *Geospatial Analysis A Comprehensive Guide to Principles Techniques and Software Tools* (6th ed.). Retrieved from https://www.spatialanalysisonline.com/HTML/index.html

Dobbs, C., Hernández-Moreno, Á., Reyes-Paecke, S., & Miranda, M. D. (2018). Exploring temporal dynamics of urban ecosystem services in Latin America: The case of Bogota (Colombia) and Santiago (Chile). *Ecological Indicators*, *85*(November 2017), 1068–1080. https://doi.org/10.1016/j.ecolind.2017.11.062

Escobar Franco, L. F. (2012). Plan Ambiental Local Kennedy 2013-2016. *Alcaldía Local de Kennedy*, 1–68. Retrieved from http://ambientebogota.gov.co/documents/10157/2883162/PAL+Kennedy+2013-2016.pdf

Estoque, R. C., & Murayama, Y. (2017). Monitoring surface urban heat island formation in a tropical mountain city using Landsat data (1987–2015). *ISPRS Journal of Photogrammetry and Remote Sensing*, *133*, 18–29. https://doi.org/10.1016/j.isprsjprs.2017.09.008

Ezimand, K., Kakroodi, A. A., & Kiavarz, M. (2018). The development of spectral indices for detecting built-up land areas and their relationship with land-surface temperature. *International Journal of Remote Sensing*, *39*(23), 8428–8449. https://doi.org/https://doi.org/10.1080/01431161.2018.1488282

Ezimand, K., Chahardoli, M., Azadbakht, M., & Matkan, A. A. (2021). Spatiotemporal analysis of land surface temperature using multi-temporal and multi-sensor image fusion techniques. *Sustainable Cities and Society*, *64*(March 2020), 102508. https://doi.org/10.1016/j.scs.2020.102508

Gaudencio, Ramos Niembro Fiscal Escalante, R., Maqueda Zamora, M., Sada Gámiz, J., & Horacio, B. S. (1999). *Variables que influyen en el consumo de energía eléctrica*. Retrieved from https://www.ineel.mx/publica/boletin-ef99/aplief99.htm

Grigoraș, G., & Urițescu, B. (2019). Land Use/Land Cover changes dynamics and their effects on Surface Urban Heat Island in Bucharest, Romania. *International Journal of Applied Earth*

Observation and Geoinformation, *80*(March), 115–126. https://doi.org/10.1016/j.jag.2019.03.009

Grover, A., & Singh, R. B. (2015). Analysis of urban heat island (UHI) in relation to normalized difference vegetation index (ndvi): A comparative study of Delhi and Mumbai. *Environments - MDPI*, *2*(2), 125–138. https://doi.org/10.3390/environments2020125

Gunawardena, K., Kershaw, T., & Steemers, K. (2019). Simulation pathway for estimating heat island influence on urban/suburban building space-conditioning loads and response to facade material changes. *Building and Environment*, *150*(January), 195–205. https://doi.org/10.1016/j.buildenv.2019.01.006

Guzman, L. A., Gomez, A. M., & Rivera, C. (2017). A Strategic Tour Generation Modeling within a Dynamic Land-Use and Transport Framework: A Case Study of Bogota, Colombia. *Transportation Research Procedia*, *25*, 2536–2551. https://doi.org/10.1016/j.trpro.2017.05.292

Ihlen, V., & USGS. (2019a). *Landsat 7 (L7) Data Users Handbook* (p. 151). p. 151. Retrieved from https://landsat.usgs.gov/sites/default/files/documents/LSDS-1927_L7_Data_Users_Handbook.pdf

Ihlen, V., & USGS. (2019b). *Landsat 8 (L8) Data Users Handbook* (p. 114). p. 114. Retrieved from https://landsat.usgs.gov/documents/Landsat8DataUsersHandbook.pdf

Kao, J Y; Kelley, G. E. (1996). Factors affecting the energy consumption of two refrigerator-freezers. *ASHRAETransaction*, *102*(2), 525–545.

Kaur, R., & Pandey, P. (2022). A review on spectral indices for built - up area extraction using remote sensing technology. *Arabian Journal of Geosciences*. https://doi.org/10.1007/s12517-022-09688-x

Kikon, N., Singh, P., Singh, S. K., & Vyas, A. (2016). Assessment of urban heat islands (UHI) of Noida City, India using multi-temporal satellite data. *Sustainable Cities and Society*, *22*, 19–28. https://doi.org/10.1016/j.scs.2016.01.005

Litardo, J., Palme, M., Borbor-Cordova, M., Caiza, R., Macias, J., Hidalgo-Leon, R., & Soriano, G. (2020). Urban Heat Island intensity and buildings' energy needs in Duran, Ecuador: Simulation studies and proposal of mitigation strategies. *Sustainable Cities and Society*, *62*(July), 102387. https://doi.org/10.1016/j.scs.2020.102387

Liu, X., Zhou, Y., Yue, W., Li, X., Liu, Y., & Lu, D. (2020). Spatiotemporal patterns of summer urban heat island in Beijing, China using an improved land surface temperature. *Journal of Cleaner Production*, *257*, 120529. https://doi.org/10.1016/j.jclepro.2020.120529

Madanian, M., Soffianian, A. R., Soltani Koupai, S., Pourmanafi, S., & Momeni, M. (2018). The study of thermal pattern changes using Landsat-derived land surface temperature in the central part of Isfahan province. *Sustainable Cities and Society*, *39*(November 2017), 650–661. https://doi.org/10.1016/j.scs.2018.03.018

Min, M., Lin, C., Duan, X., Jin, Z., & Zhang, L. (2019). Spatial distribution and driving force analysis of urban heat island effect based on raster data: A case study of the Nanjing metropolitan area, China. *Sustainable Cities and Society*, *50*(December 2018), 101637. https://doi.org/10.1016/j.scs.2019.101637

Molina Jaramillo, A. N. (2018). Território, espaços e saúde: Redimensionar o espaço em saúde pública. *Cadernos de Saude Publica*, *34*(1), 1–12. https://doi.org/10.1590/0102-311x00075117

Musse, M. A., Barona, D. A., & Santana Rodriguez, L. M. (2018). Urban environmental quality assessment using remote sensing and census data. *International Journal of Applied Earth Observation and Geoinformation*, *71*, 95–108. https://doi.org/10.1016/j.jag.2018.05.010

Ngarambe, J., Joen, S. J., Han, C. H., & Yun, G. Y. (2021). Exploring the relationship between particulate matter, CO, SO2, NO2, O3 and urban heat island in Seoul, Korea. *Journal of Hazardous Materials*, *403*(2), 123615. https://doi.org/10.1016/j.jhazmat.2020.123615

Oke, T. R. (1982). The energetic basis of the urban heat island (Symons Memorial Lecture, 20 May 1980). *Quarterly Journal, Royal Meteorological Society*, *108*(455), 1–24.

Oke, T. R. (1988). The urban energy balance. *Progress in Physical Geography*, *12*(4), 471–508.

https://doi.org/10.1177/030913338801200401
Papparelli, A., Kurbán, A., & Cúnsulo, M. (2011). Isla de calor y ocupación espacial urbana en San Juan, Argentina: análisis evolutivo. *Cuadernos de Vivienda y Urbanismo*, *4*(7), 110–120.
Parvez M.I., A. Y. A. (2019). Exploring the Influence of Land Use Type and Population Density on Urban Heat Island Intensity. *Advances in Remote Sensing and Geo Informatics Applications. CAJG 2018. Advances in Science, Technology & Innovation (IEREK Interdisciplinary Series for Sustainable Development)*, 113–115. https://doi.org/https://doi.org/10.1007/978-3-030-01440-7_27
Peres, L. de F., Lucena, A. J. de, Rotunno Filho, O. C., & França, J. R. de A. (2018). The urban heat island in Rio de Janeiro, Brazil, in the last 30 years using remote sensing data. *International Journal of Applied Earth Observation and Geoinformation*, *64*(October 2016), 104–116. https://doi.org/10.1016/j.jag.2017.08.012
Portela, C. I., Massi, K. G., Rodrigues, T., & Alcântara, E. (2020). Impact of urban and industrial features on land surface temperature: Evidences from satellite thermal indices. *Sustainable Cities and Society*, *56*(February), 102100. https://doi.org/10.1016/j.scs.2020.102100
Ramírez-Aguilar, E. A., & Lucas Souza, L. C. (2019). Urban form and population density: Influences on Urban Heat Island intensities in Bogotá, Colombia. *Urban Climate*, *29*(May), 100497. https://doi.org/10.1016/j.uclim.2019.100497
Rizwan, A. M., Dennis, L. Y. C., & Liu, C. (2008). A review on the generation, determination and mitigation of Urban Heat Island. *Journal of Environmental Sciences*, *20*(1), 120–128. https://doi.org/10.1016/S1001-0742(08)60019-4
SDA. (2020). *Informe Anual de Calidad del aire de Bogotá - 2019*. 1–201. Retrieved from http://rmcab.ambientebogota.gov.co/Pagesfiles/IA 200531 Informe Anual de Calidad del Aire Año 2019.pdf
SDP. (2020). *Proyecciones de población*. Retrieved from http://www.sdp.gov.co/sites/default/files/visor_proyecciones_sdp_v1.1_0.xlsm
Senanayake, I. P., Welivitiya, W. D. D. P., & Nadeeka, P. M. (2013). Remote sensing based analysis of urban heat islands with vegetation cover in Colombo city, Sri Lanka using Landsat-7 ETM+ data. *Urban Climate*, *5*, 19–35. https://doi.org/10.1016/j.uclim.2013.07.004
Shen, L., Kyllo, J., & Guo, X. (2013). An Integrated Model Based on a Hierarchical Indices System for Monitoring and Evaluating Urban Sustainability. *Sustainability*, *5*(2), 524–559. https://doi.org/10.3390/su5020524
Singh, P., Kikon, N., & Verma, P. (2017). Impact of land use change and urbanization on urban heat island in Lucknow city, Central India. A remote sensing based estimate. *Sustainable Cities and Society*, *32*, 100–114. https://doi.org/10.1016/j.scs.2017.02.018
Soltani, A., & Sharifi, E. (2017). Daily variation of urban heat island effect and its correlations to urban greenery: A case study of Adelaide. *Frontiers of Architectural Research*, *6*(4), 529–538. https://doi.org/10.1016/j.foar.2017.08.001
Ulpiani, G. (2021). On the linkage between urban heat island and urban pollution island: Three-decade literature review towards a conceptual framework. *Science of the Total Environment*, *751*, 141727. https://doi.org/10.1016/j.scitotenv.2020.141727
UN-Habitat. (2019). *Implementación de la Agenda 2030 y la Nueva Agenda Urbana*. Retrieved from https://www.aciamericas.coop/xxiconferencia/wp-content/uploads/2019/12/05_Quintana-ONU-Habitat.pdf
UNDP. (2020). Goal 11: Sustainable cities and communities. Retrieved November 11, 2020, from https://www.undp.org/content/undp/en/home/sustainable-development-goals/goal-11-sustainable-cities-and-communities.html#targets
United Nations. (2007). *Indicators of Sustainable Development: Guidelines and Methodologies* (3th ed.). https://doi.org/10.1016/j.cirpj.2010.03.002
United Nations. (2019). *World urbanization prospects The 2018 Revision*. https://doi.org/10.18356/b9e995fe-en

Veeduría Distrital. (2018). *Kennedy: Ficha Local*. Retrieved from https://www.veeduriadistrital.gov.co/sites/default/files/files/Ficha Localidad Kennedy.pdf

Wang, S., Ma, Q., Ding, H., & Liang, H. (2018). Detection of urban expansion and land surface temperature change using multi-temporal landsat images. *Resources, Conservation and Recycling*, *128*, 526–534. https://doi.org/10.1016/j.resconrec.2016.05.011

WHO. (2006). *WHO Air quality guidelines for particulate matter, ozone, nitrogen dioxide and sulfur dioxide. Global update 2005*. Retrieved from https://apps.who.int/iris/bitstream/handle/10665/69477/WHO_SDE_PHE_OEH_06.02_eng.pdf;jsessionid=54263785E93420048269696C80477B40?sequence=1

Wu, X., Wang, G., Yao, R., Wang, L., Yu, D., & Gui, X. (2019). Investigating surface urban heat islands in South America based on MODIS data from 2003-2016. *Remote Sensing*, *11*, 1212. https://doi.org/10.3390/rs11101212

Xu, H. (2006). Modification of normalized difference water index (NDWI) to enhance open water features in remotely sensed imagery. *International Journal of Remote Sensing*, *27*(14), 3025–3033. https://doi.org/10.1080/01431160600589179

Yao, L., Sun, S., Song, C., Li, J., Xu, W., & Xu, Y. (2021). Understanding the spatiotemporal pattern of the urban heat island footprint in the context of urbanization , a case study in Beijing , China. *Applied Geography*, *133*(June), 102496. https://doi.org/10.1016/j.apgeog.2021.102496

Yuan, F., & Bauer, M. E. (2007). Comparison of impervious surface area and normalized difference vegetation index as indicators of surface urban heat island effects in Landsat imagery. *Remote Sensing of Environment*, *106*(3), 375–386. https://doi.org/10.1016/j.rse.2006.09.003

Yue, W., Liu, Y., & Fan, P. (2012). *Assessing spatial pattern of urban thermal environment in Shanghai , China*. 899–911. https://doi.org/10.1007/s00477-012-0638-1

Yunda, J. G., & Sletto, B. (2020). Densification, private sector-led development, and social polarization in the global south: Lessons from a century of zoning in Bogotá. *Cities*, *97*(October 2019), 102550. https://doi.org/10.1016/j.cities.2019.102550

Zha, Y., Gao, J., & Ni, S. (2003). Use of normalized difference built-up index in automatically mapping urban areas from TM imagery. *International Journal of Remote Sensing*, *24*(3), 583–594. https://doi.org/10.1080/01431160304987

Zhang, X., Estoque, R. C., & Murayama, Y. (2017). An urban heat island study in Nanchang City, China based on land surface temperature and social-ecological variables. *Sustainable Cities and Society*, *32*(May), 557–568. https://doi.org/10.1016/j.scs.2017.05.005

Zhou, D., Xiao, J., Bonafoni, S., Berger, C., Deilami, K., Zhou, Y., … Sobrino, J. A. (2019). Satellite remote sensing of surface urban heat islands: Progress, challenges, and perspectives. *Remote Sensing*, *11*(1), 1–36. https://doi.org/10.3390/rs11010048